Journal of Fluorescence, Vol. 6, No. 3, 1996

Resolution of Multiexponential Spectral Relaxation of Y_t-Base by Global Analysis of Collisionally Quenched Samples[1]

Henryk Szmacinski,[2] Ignacy Gryczynski,[2] and Joseph R. Lakowicz[2]

Received June 1, 1995; accepted July 26, 1996

We measured the wavelength-dependent intensity decays of 4,9-dihydro-4,6-dimethyl-9-oxo-1*H*-imidazo-1,2*a*-purine (Y_t-base) in propanol to determine the time-resolved emission spectra and rates of spectral relaxation. We found that resolution of the spectral relaxation times was dramatically improved by global analysis of the frequency-domain data with increasing amounts of the collisional quencher CCl_4. Collisional quenching preferentially decreases the longer-lived relaxed component of the emission, thereby increasing the fractional contribution of the incompletely relaxed portion of the emission. The data could not be explained by a single spectral relaxation time, and at least two relaxation times are needed to describe the time-dependent emission center of gravity of Y_t-base.

KEY WORDS: Frequency-domain fluorometry; fluorescence decay; solvent effects; solvent relaxation; time-resolved emission spectra.

INTRODUCTION

The fluorescence emission of molecules in condensed phase is invariably shifted to longer wavelengths relative to their absorption spectra. This phenomenon, known as the Stokes' shift, has been known since its initial observation by Professor G. Stokes in 1852.[1] The magnitude of the Stokes' shift depends upon molecular interactions between the fluorophore and the solvent. Factors influencing the Stokes' shift include solvent polarity, viscosity, and extent of hydrogen bonding. In spite of considerable efforts to explain these spectra shifts quantitatively, most theories for solvent effects rely on continuum approximations which ignore the detailed solvent–fluorophore interactions.[2–6] However, there have been attempts to incorporate additional details about the solvents into the theory.[7,8]

An important aspect of the Stokes' shift, or spectral relaxation, is that the extent of spectral relaxation depends upon the relative value of the fluorescence decay time (τ) and the spectral relaxation time (τ_R). In highly viscous solvents, emission typically occurs prior to reorganization of the solvent around the excited-state dipole, whereas solvent relaxation is often complete in more fluid solvents. Hence, under appropriate conditions, time-dependent decays are expected to depend on emission wavelength,[9–11] as confirmed by early studies of time-dependent spectral relaxation.[12,13]

The use of time-dependent spectral relaxation has been extended to biological macromolecules. In pioneering studies of lipid bilayers, Brand and co-workers[14,15] used time-correlated single—photon counting (TCSPC) to determine the time-resolved emission spectra (TRES) of labeled membranes. Several years later it was found that TRES could also be obtained from the frequency-domain data.[16] The time-resolved emission

[1] Dedicated to Professor Stefan Paszyc on the occasion of his 70th birthday.

[2] Center for Fluorescence Spectroscopy, Department of Biochemistry and Molecular Biology, University of Maryland, School of Medicine, 108 North Greene Street, Baltimore, Maryland 21201.

1053-0509/96/0900-0177$09.50/0

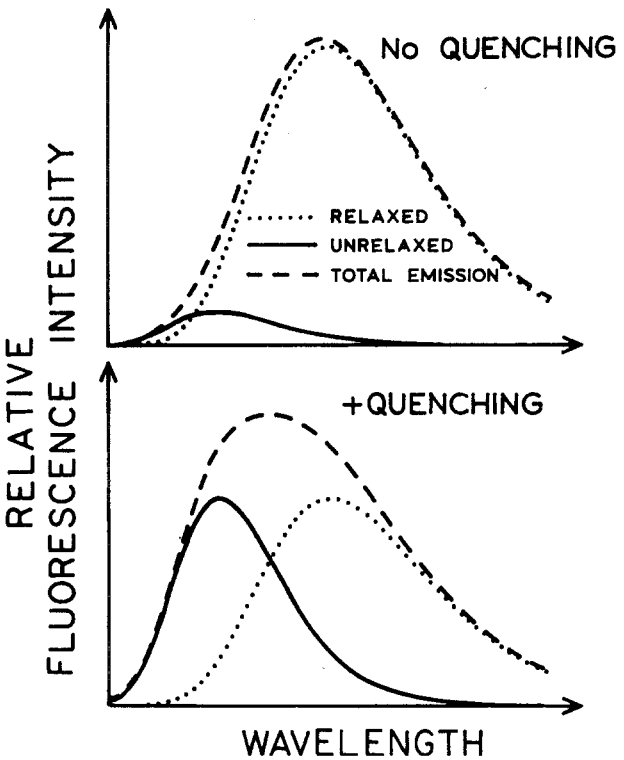

Scheme I. Intuitive description of the effects of collisional quenching with time-dependent spectral relaxation.

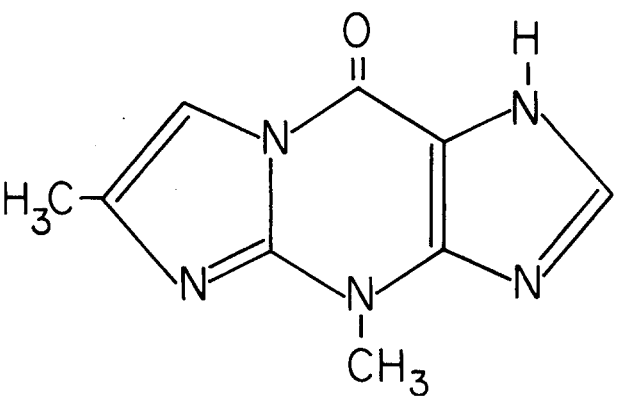

Scheme II. Chemical structure of Y_t-base.

spectra are known to be a sensitive indicator of biopolymer dynamics.

In recent years there has been a renewed interest in the use of time-resolved emission spectroscopy in chemical physics.[17,18] This interest has resulted form the recognition that detailed information on solvent dynamics of solvents is contained within the time-dependent data.[19–21] Additionally, the opportunity to obtain quantitative data has improved due to the use of picosecond (ps) and femtosecond (fs) lasers to study solvent relaxation,[22,23] and one can compare the data with molecular dynamic calculations.[22–24] To date, most experimental studies of spectral relaxation have found evidence for multiple relaxation times.[27–29] Resolution of multiple relaxation times is of interest because they reflect the dynamic response of the solvent to the instantaneous perturbation of fluorophore excitation. However, resolution of the spectral relaxation times is hindered by the complexity of the process. In moderately fluid solvents, the emission is dominately from the relaxed species.

In the present report, we describe a method to improve the resolution of the spectral relaxation. As usual, the time-resolved data are collected across the emission spectra. Under our experimental conditions, the emission is mostly from the solvent relaxed state (Scheme I, top, dotted line). Additionally, similar data are collected in the presence of a collisional quencher. The process of quenching preferentially decreases the contribution of the relaxed state to the total emission, so that the emission from the unrelaxed state makes a larger contribution to the emission (Scheme I, bottom, solid line). The lifetime of the unrelaxed state is short because this state is depopulated both by emission and by spectral relaxation. The relaxed state is preferentially quenched because it displays a longer mean lifetime. The time-resolved data for the quenched solutions thus contain an increased fraction of the emission from the incompletely relaxed state. Global analysis of the time-resolved data for the unquenched and quenched solutions was shown to allow determination of two spectral relaxation times of 4,4-dihydro-4,6-dimethyl-9-oxo-1*H*-imidazo-1,2*a*-purine (Y_t-base) (Scheme II) in an alcoholic solvent. The time-resolved emission center of gravity of Y_t-base was found to display a double-exponential time-dependent spectral shift. The approach of using global analysis of quenched and unquenched samples has been used previously to evaluate various kinetic models for excited-state reactions[30] and to study distance distributions in the presence of diffusion.[31]

MATERIALS AND METHODS

The frequency-domain intensity decays were measured using a 2-GHz harmonic content fluorometer.[32] The excitation wavelength was 310 nm from the frequency-doubled output of a rhodamine 6G dye laser. The instrument provides phase and modulation data with similar uncertainties over its entire frequency range. Magic-angle polarizer orientations were used to eliminate the effects of rotational diffusion. The emission was observed through a series of interference filters from 360

to 520 nm, each with a 10-nm bandpass. The Y_t-base was prepared by reacting 3-methylguanine with bromoacetone[33,34] and was purified by HPLC before the measurements. All measurements were made in *n*-propanol at −20°C. There was no significant loss of intensity or changing phase or modulation values during the experiment, suggesting that photodecomposition was not significant.

THEORY

Time-resolved emission can be calculated from the intensity decays $[I(\lambda, t)]$ measured for wavelengths (λ) spanning the emission.[15] In our case, we measured the frequency response of the emission, which provides wavelength-dependent values for the phase angle $[\theta_\omega(\lambda)]$ and the modulation $[m_\omega(\lambda)]$, at various frequencies (ω). The phase and modulation values are used with nonlinear least-squares[35,36] to calculate the impulse response at each wavelength in terms of the multiexponential model

$$I^Q(\lambda, t) = \sum_i \alpha_i^Q(\lambda) \exp(-t/\tau_i^Q) \tag{1}$$

In this expression, Q indicates the quencher concentration, and α_i, the preexponential factor associated with the ith decay time τ_i^Q. The decay times are assumed to be independent of emission wavelength. The multiexponential decay components are determined as usual from least-squares analysis.[35,36]

The objective is to determine the parameters describing the time-dependent decrease in the emission center of gravity, $\bar{\nu}(t)$. For a single spectral relaxation time

$$\bar{\nu}(t) = \bar{\nu}_\infty + (\bar{\nu}_0 - \bar{\nu}_\infty) \exp(-t/\tau_R) = \bar{\nu}_\infty + \Delta\bar{\nu} \exp(-t/\tau_R) \tag{2}$$

where $\bar{\nu}_0$ and $\bar{\nu}_\infty$ are the values in wavenumbers at t = 0 and infinity, respectively, and τ_R is the spectral relaxation time. For the system described in this report, the relaxation was found to be more complex than a single exponential. Hence, we used a multiexponential relaxation model with up to two relaxation times, where $\Delta\nu_j$ is the spectral shift associated with the j relaxation time τ_{Rj}.

$$\bar{\nu}(t) = \bar{\nu}_\infty + \sum_j^2 \Delta\bar{\nu}_j \exp(-t/\tau_{Rj}) \tag{3}$$

At any time t, the center of gravity can be calculated from the properly normalized impulse response functions, $I_N^Q(\lambda, t)$. The normalization factor is given by[15]

$$H^Q(\lambda) = \frac{F^Q(\lambda)}{\sum_i \alpha_i^Q(\lambda)\, \tau_i^Q} \tag{4}$$

where $F^Q(\lambda)$ is the peak-normalized steady-state emission spectrum. The normalized values of $\alpha_i^Q(\lambda)$ are

$$\alpha_{Ni}^Q(\lambda) = H^Q(\lambda)\alpha_i^Q(\lambda) \tag{5}$$

and

$$I_N^Q(\lambda, t) = H^Q(\lambda) I^Q(\lambda, t) \tag{6}$$

The time-dependent center of gravity $\bar{\nu}(t)$ is proportional to the average energy of the emission. For data collected at equal wavelength intervals and a constant bandpass (nm), the center of gravity (in kK; 1 kK = $10^3 cm^{-1}$) is calculated using

$$\bar{\nu}(t) = 10{,}000 \frac{\sum_{\lambda,Q} I_N^Q(\lambda, t)\lambda^{-1}}{\sum_{\lambda,Q} I_N^Q(\lambda, t)} \tag{7}$$

where the sum extends over the wavelengths (λ) and quencher concentrations (Q).

The parameters which characterized the rates and extents of spectral relaxation (τ_{Rj}, $\Delta\nu_j$, $\bar{\nu}_\infty$) are obtained by nonlinear least-squares fitting of the time-dependent center of gravity $\bar{\nu}(t)$ values from Eq. (7) to the calculated values $\bar{\nu}^c(t)$ from Eqs. (2) and (3). The parameter values (τ_{Rj}) and ($\Delta\bar{\nu}_j$) are varied to yield the minimum values of χ_R^2,

$$\chi_R^2 = \frac{1}{k} \sum_{t,Q} \left(\frac{\bar{\nu}(t) - \bar{\nu}^c(t)}{\delta\bar{\nu}} \right)^2 \tag{8}$$

where k is the number of degrees of freedom and $\delta\bar{\nu}$ is the estimated error in $\bar{\nu}(t)$, which was taken to be from 0.003 to 0.008 kK. The measurements at each quencher concentration may result in somewhat different values of $\bar{\nu}(t)$, which reflect the complex nature of the relaxation and an incomplete resolution of the spectral decay using any one set of data. For the unquenched sample (long mean decay time) better resolution is obtained for longer relaxation time, and for a highly quenched sample (short mean decay time) the shorter relaxation time can be determined. For the present analyses we used global fits to all the data and recovered a single set of spectral relaxation parameters.

RESULTS

Emission spectra of Y_t-base in propanol at −20°C are shown in Fig. 1. The solvent and temperature were selected to provide a solvent of adequate fluidity for dif-

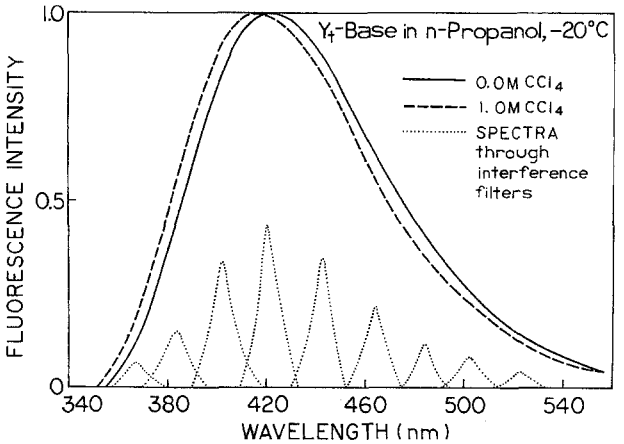

Fig. 1. Emission spectra of Y_t-base in *n*-propanol at −20°C in the absence (—) and presence (– – –) of 1.0 *M* CCl_4. Also shown are the spectra through the filters used to measure the wavelength-dependent frequency-domain data.

fusion of the collisional quencher CCl_4, while still displaying rates of spectral relaxation on the ps to ns time scale. Solutions of Y_t-base were examined without CCl_4 and with 0.5 and 1.0 *M* CCl_4. In the latter case, the steady-state emission spectrum of Y_t-base is shifted to shorter wavelengths by 4 to 5 nm. In the polar proposed solvent there are 4.8% (0.5 *M* CCl_4) and 9.6% (1.0 *M*) (v/v) of nonpolar CCl_4. It has been shown that low concentrations (less than 20%) of nonpolar solvents in mixtures with a polar solvent have a very small effect on the spectral properties of Y_t-base.[37] This spectral shift is due to a decrease in the mean decay time due to collisional quenching. Such effects have been observed previously for indole in ethanol,[38] and for probes bound to membranes,[39] and are expected when the decay time is shortened to a value comparable to the spectral relaxation time.

We measured the frequency-domain intensity decays of Y_t-base at 20-nm intervals across its emission spectrum. The transmission profiles of these interference filters are shown in Fig. 1. The transmission bandwidths near 10 nm provide adequate resolution for the broad emission spectrum of Y_t-base. The frequency responses were markedly different on the blue (360-nm) and red (500- or 520-nm) sides of the emission (Fig. 2). The differences reflect the rate of spectral relaxation. The phase angles are larger, and the modulation smaller, on the long-wavelength side of the emission, which is typical of a fluorophore which displays a time-dependent spectral shift or an excited-state reaction.[40] It should be noted that the presence of static quenching would not affect the results because the statically quenched fluorophores will not contribute to the intensity decay.

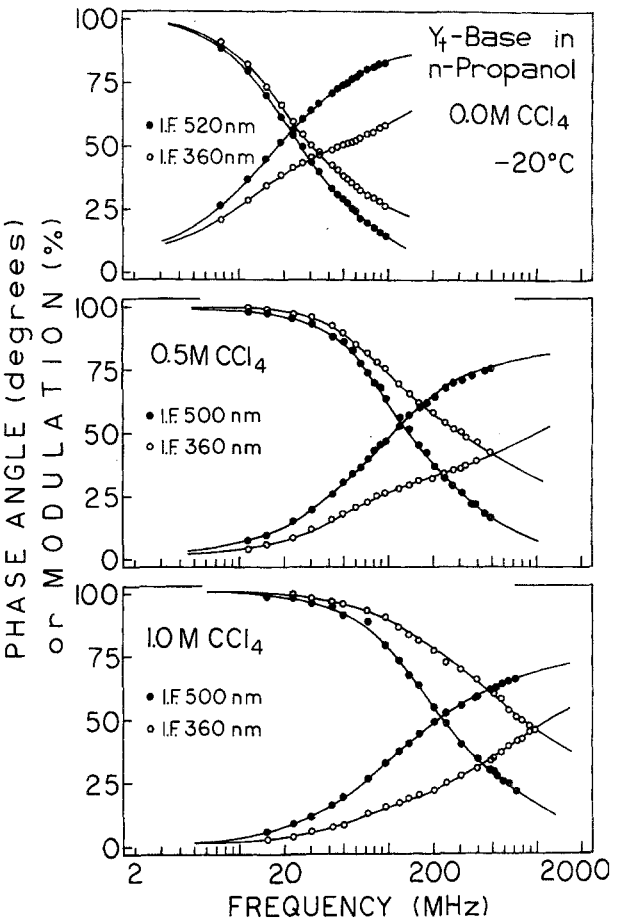

Fig. 2. Frequency-domain intensity decays of Y_t-base on the blue (360-nm) and red (500- or 520-nm) sides of the emission.

The multiexponential analysis of these data are summarized in Table I, for 0, 0.5, and 1.0 *M* CCl_4. In this analysis, the decay times were global variables, the same for all emission wavelengths. The amplitudes were allowed to vary at each wavelength as nonglobal parameters. The intensity decay could not be fit to a single decay time, as seen from the elevated χ_R^2 values in Table I. The data were analyzed in terms of a double-exponential decay, but we note that this analysis provides only an approximate representation of what is likely to be a more complex decay law. In particular, we have demonstrated that collisional quenching results in complex nonexponential intensity decays due to transient effects in diffusion[41] and due to a distance-dependent rate of quenching.[42] Nonetheless, for the purpose of calculating the time-resolved emission spectra, the double-exponential model provides an adequate representation of the time-dependent decays. The contributions of the decay times at each emission wavelength can be seen from

Table I. Global Analysis of the Intensity Decay of Y_t-Base in Propanol at −20°C

Wavelength (nm)	α_1	f_1	α_2	f_2	χ^2_R
0 *M* CCl_4	τ_1 = 1.55 ns[a]		τ_2 = 10.46 ns[a]		
360	0.660	0.224	0.340	0.776	
380	0.337	0.070	0.663	0.930	
400	0.156	0.027	0.844	0.973	
420	0.066	0.010	0.934	0.990	
440	0.026	0.004	0.974	0.996	
460	0.000	0.000	1.000	1.000	
480	−0.017[b]	−0.002	0.983	1.002[b]	
500	−0.047	−0.007	0.953	1.007	
520	−0.083	−0.013	0.917	1.013	1.3[c](566.3)[d]
0.5 *M* CCl_4	τ_1 = 0.23 ns		τ_2 = 1.96 ns		
360	0.872	0.445	0.128	0.555	
380	0.671	0.193	0.329	0.807	
400	0.531	0.117	0.469	0.883	
420	0.368	0.064	0.632	0.936	
440	0.292	0.046	0.708	0.954	
460	0.217	0.031	0.783	0.969	
480	0.202	0.029	0.798	0.971	
500	0.180	0.025	0.820	0.975	2.3 (1199)
1 *M* CCl_4	τ_1 = 0.17 ns		τ_2 = 1.25 ns		
360	0.926	0.626	0.074	0.374	
380	0.722	0.314	0.278	0.686	
400	0.663	0.209	0.337	0.791	
420	0.582	0.158	0.418	0.842	
440	0.523	0.129	0.477	0.871	
460	0.518	0.126	0.482	0.874	
480	0.479	0.110	0.521	0.890	
500	0.463	0.102	0.537	0.898	6.9 (1794.5)

[a] Decay times from the global analysis for all wavelengths.
[b] The values of α_1 and α_2 obtained using normalization $|\alpha_1| + \alpha_2 = 1.0$ and $f_1 + f_2 = 1.0$.
[c] The χ^2_R values were calculated using $\delta\phi = 0.2°$ and $\delta m = 0.005$ as the uncertainties in the phase and modulation, respectively.
[d] The numbers in parentheses are the χ^2_R values obtained for the single-decay time fits.

the fractional intensities. The fractional intensity of the long decay-time term (f_2) increased with emission wavelength (Table I). However, we note that in the presence of an excited-state reaction the f_i values do not represent the relative intensities of the individual states. In the absence of CCl_4, we found a component with a negative preexponential factor on the red side of the emission. Such a component clearly demonstrates that this fraction of the emission results from an excited-state process, that is, formation of a product subsequent to formation of the initially excited state.[43–45] These large phase angles result from molecules in the relaxed state which formed subsequent to excitation from molecules excited into the unrelaxed state. An important feature of the phase-modulation data for an excited-state process is the observation of apparent phase lifetimes (τ_p) which are longer than the modulation lifetimes (τ_m) on the long-wavelength side of the emission. We observed higher values of τ_p than τ_m at wavelengths of 460 nm and longer. At 520 nm the phase lifetime is τ_p = 14.44 ns, and the modulation lifetime is τ_m = 11.10, for a modulation frequency of 94.875 MHz. For multiexponential decay without an excited-state reaction, one observes that $\tau_p < \tau_m$. In the presence of 0.5 and 1.0 *M* CCl_4, the negative component is no longer found in the global analysis (Table I). For the quenched samples it is difficult to distinguish spectral relaxation from heterogeneity of fluorescence decay. This difficulty is probably also a result of the large degree of spectral overlap of the unrelaxed and relaxed emission.

The results of the multiexponential analysis were used to calculate the time-resolved emission spectra. Typical time-resolved emission spectra are shown in Fig. 3. The spectra are seen to shift progressively to longer wavelengths as time increases. The most red-shifted TRES is seen at 3.0 ns in the absence of CCl_4 (top). The most blue-shifted TRES is seen at 5 ps with 1 *M* CCl_4 (bottom). It is interesting that at 5 ps, in the absence of CCl_4, the apparent TRES is less blue-shifted than the TRES with 1.0 *M* CCl_4. The discrepancy reflects the lack of resolution at short times in the absence of the collisional quencher. Stated alternatively, the addition of the collisional quencher results in an improved ability to detect the emission spectrum of Y_t-base existing at earlier times following excitation.

The data for Y_t-base, with three concentrations of CCl_4 (0, 0.5, and 1.0 *M*), were analyzed globally to obtain a single set of time-dependent center of gravity data (Fig. 4). These data were then analyzed to obtain the best fit to the single- and double-relaxation time models, Eqs. (2) and (3), respectively. The data were not consistent with a single spectral relaxation time, as can be seen from the poor match between the experimental data (●) and the model (– – –). Additionally, the deviations from the single relaxation time model (○; bottom) vary systematically, which is usually indicative of an inadequate fit. In contrast, the data are consistent with a two-relaxation time model (Fig. 4, ——), which also results in more random deviations (●; bottom).

The advantage of global analysis of progressively quenched samples is shown in Table II, which summarizes the one- and two-relaxation time analysis of the time-dependent values of the emission center of gravity. In the absence of the collisional quencher, the data were

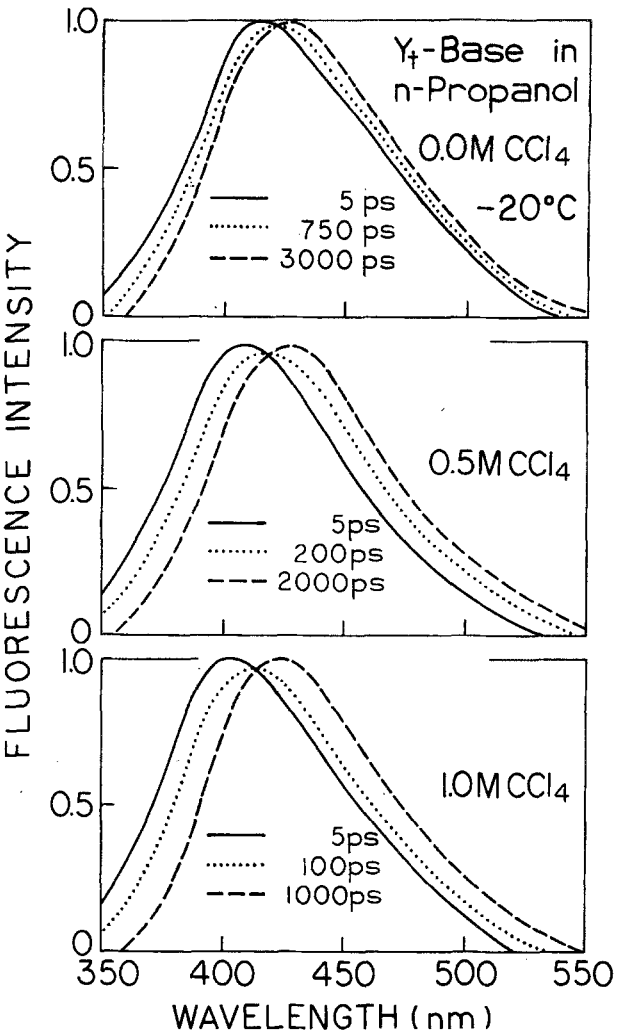

Fig. 3. Time-resolved emission spectra of Y_t-base in *n*-propanol at −20°C.

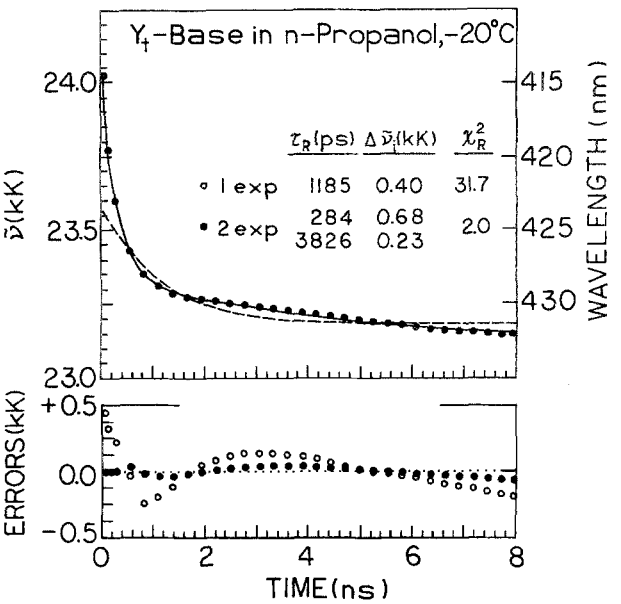

Fig. 4. Time-dependent emission center of gravity for Y_t-base in *n*-propanol at −20°C.

Table II. Spectral Relaxation Parameters for Y_t-Base in Propanol at −20°C

CCl_4 (*M*)	Model	$\Delta\bar{\nu}_i$ (kK)	τ_R (ps)	χ^2_R
0	1 exp	0.34	1920	2.68
	2 exp	—	—	2.68
		—	—	
0.5	1 exp	0.78	396	1.98
	2 exp	—	393	2.01
		—	399	
1.0	1 exp	0.78	355	2.50
	2 exp	0.11	41	1.18
		0.70	445	
Global: 0, 0.5, and 1.0	1 exp	0.40	1185	31.7
	2 exp	0.68	284	
		0.23	3826	2.0

not adequate to recover two spectral relaxation times. This can be seen from the similarity of the χ^2_R values for the one- and two-relaxation time fits (Table II). In contrast, global analysis in the presence of CCl_4 results in a 16-fold decrease in χ^2_R for the two-relaxation time model, compared to the single-relaxation time model. While the actual relaxation may be still more complex, the results of the global analysis indicate the improved resolution of spectral relaxation obtainable with collisional quenching, in agreement with an earlier report.[30]

To evaluate further the resolution of the spectral relaxation times, we examined the χ^2_R surfaces (Fig. 5). These surfaces were calculated by holding one of the relaxation times fixed at the value shown on the *z*-axis, while the other parameters ($\Delta\bar{\nu}_1$, $\Delta\bar{\nu}_2$, and τ_{R1} or τ_{R2}) were varied to obtain the minimum value of χ^2_R. For the data measured for a single quencher concentration (0 or 1 *M* CCl_4) the χ^2_R minima are barely visible, which indicates that the values of τ_{R1} and τ_{R2} are not determined from the data. In contrast, well-defined χ^2_R minima were found for global analysis of the frequency-domain data without and with CCl_4. Based on these χ^2_R surfaces, we judge that the spectral relaxation times are 284 ± 20 and 3826 ± 100 ps. These χ^2_R surfaces demonstrate the value of global analysis with quenching for recovery of complex spectral decay kinetics.

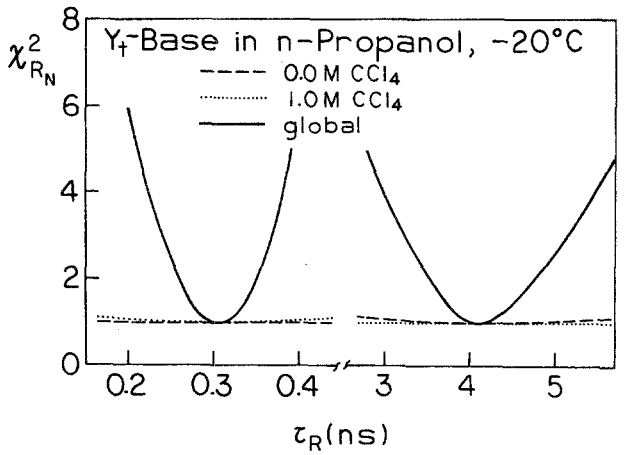

Fig. 5. χ^2 surfaces for the spectral relaxation times of Y_t-base in *n*-propanol at −20°C.

DISCUSSION

What is the origin of the improved resolution of spectral decay kinetics with collisional quenching? In our opinion, there are two reasons. First, the use of collisional quenching shortens the mean decay time of the sample. In the frequency domain, a shorter lifetime results in the ability to measure the frequency response to higher modulation frequencies. This effect can be seen in Fig. 2. In the absence of quenching, the frequency response could be measured only to 200 MHz. In the presence of quenching, the data were measurable to 2 GHz. These higher-frequency measurements reflect short-lived components (fast kinetics) in the intensity decay, some of which display the blue-shifted emission.

The second reason for improved resolution with collisional quenching is because the decay time is reduced to a value more comparable to the spectral relaxation time (Scheme I). For instance, in the absence of CCl_4, the intensity decay time of Y_t-base is near 10 ns. Consequently, spectral relaxation is mostly complete (τ_R from 0.3 to 3 ns) prior to emission. In the presence of 1 *M* CCl_4, the mean decay time is near 1 ns. Hence, a larger fraction of the total emission is from the unrelaxed state.

Note that we do not intend to indicate that short decay times are easier to measure than long decay times. Collisional quenching shortens the mean decay time of the sample, which results in more emission from the unrelaxed state. In addition to shortening the decay time, collisional quenching induces short components in the intensity decay due to transient effects in quenching. The shorter mean decay time and short decay time components both allow phase and modulation measurements to be performed to higher frequencies, which provides better resolution of fast spectral relaxation.

What is the origin of the two spectral relaxation times observed for Y_t-base in propanol? It is known from studies of dielectric relaxation that alcohols display up to three relaxation times.[46] The shortest relaxation time has been assigned to rotation of the hydroxyl group around the oxygen–carbon bond, the intermediate time to rotation of the alcohol molecules, and the longest relaxation time to rotation of a hydrogen-bonded cluster of alcohol molecules or of a single molecule after breaking of its hydrogen bond(s). From the present data we have observed two, rather than three spectral relaxation times, which probably reflects the limited resolutions of our data.

The second possible origin of the multiexponential relaxation is the nonspherical shape of the Y_t-base molecule. The Y_t-base is seen to be elongated (Scheme II), and it is known to display anisotropic rotational diffusion.[47,48] In the case of nonspherical fluorophores, spectral relaxation is expected to be a double exponential even for a single solvent relaxation time.[49] However, the predicted relaxation times for nonspherical fluorophores differ by 50% or less, so this effect is unlikely to be the origin of the 10-fold different τ_R values observed for Y_t-base.

It is of interest to compare the observed extent of spectral relaxation with that predicted from the dielectric relaxation time(s) of *n*-propanol. While the dielectric relaxation of *n*-propanol is known to display as many as three relaxation times,[46] temperature-dependent values at −20°C were not available. We used a dielectric relaxation time of 1.3 ns at −20°C from Ref. 50. The extent of spectral relaxation can be quantified by the correlation function[9]

$$C(t) = \frac{\bar{\nu}(t) - \bar{\nu}_\infty}{\bar{\nu}_0 - \bar{\nu}_\infty} \tag{9}$$

where $\bar{\nu}(t)$, $\bar{\nu}_0$, and $\bar{\nu}_\infty$ are the emission centers of gravity at times t, 0, and infinity, respectively. This plot is shown in Fig. 6, which shows that the actual extent of spectral relaxation is faster than predicted from the dielectric relaxation time τ_D.

It is important to recall that the spectral relaxation times (τ_R) are expected to be shorter than the dielectric relaxation times (τ_D) and comparable to the longitudinal relaxation time (τ_L). This value can be approximated by

$$\tau_L \simeq \tau_D \frac{\varepsilon_\infty}{\varepsilon_0} \tag{10}$$

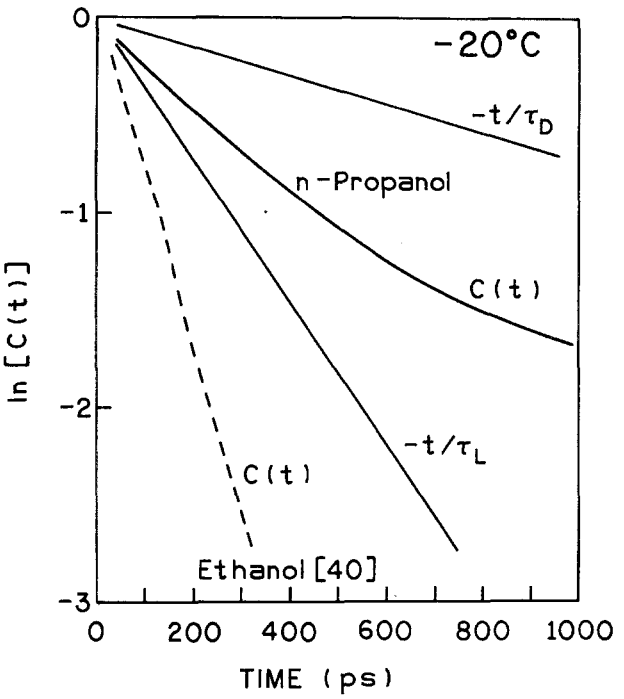

Fig. 6. Extent of spectral relaxation for Y_t -base $[C(t)]$, compared to the dielectric (τ_D) and longitudinal (τ_L) relaxation times of *n*-propanol at −20°C. Also shown is the spectral relaxation of 4,4'-(dimethylamino)phenyl sulfone (DMAPS) in ethanol at −20°C (– – –).

where ε_∞ is the refractive and ε_0 is the static dielectric constant. For propanol at −20°C, τ_D = 1.3 ns, ε_0 = 27, and ε_∞ = 5.6,[50–52] resulting in a predicted value of τ_L = 0.27 ns.

The results in Fig. 6 show that the relaxation of Y_t-base is faster than the dielectric relaxation time but slower than the longitudinal relaxation time. At early times the relaxation is more rapid, and at long times the relaxation rate appears to approach τ_D. This suggests that a variety of molecular motions is responsible for spectral relaxation of fluorophores in polar solution.

ACKNOWLEDGMENTS

This work was supported by Grants GM-39617 from the National Institutes of Health and MCB-8804931 from the National Science Foundation. The authors express appreciation to the Medical Biotechnology Center for its support.

REFERENCES

1. G. G., Stokes, *Proc. Trans. Roy. Soc. London* **142**, 463 (1852).
2. E. Von Lippert, *Z. Electrochem.* **61**, 962 (1957).
3. N. Mataga, Y. Kaifu, and M. Koizumi, *Bull. Chem. Soc. Jpn.* **29**, 465 (1956).
4. N. G. Bakhshiev, *Opt. Spectrosc.* **12**, 309 (1962).
5. L. Bilot and A. Kawski, *Z. Naturforsch.* **17a**, 621 (1962).
6. W. Liptay, *Z. Naturforsch.* **20a**, 1441 (1965).
7. R. B. MacGregor Jr. and G. Webert, *Ann. N.Y. Acad. Sci.* **366**, 140 (1981).
8. P. Suppan, *J. Photochem. Photobiol. A Chem.* **50**, 293 (1990).
9. N. G. Bakhshiev, Yu. T. Mazurenko, and I. V. Piterskaya, *Opt. Spectrosc.* **21**, 307 (1966).
10. N. G. Bakhshiev, Yu. T. Mazurenko, and I. V. Piterskaya, *Acad. Nauk USSR Bull. Phys. Sci.* **32**, 1262 (1969).
11. Yu. T. Mazurenko and N. G. Bakhshiev, *Opt. Spectrosc.* **28**, 490 (1970).
12. T. V. Veselova, L. A. Limareva, A. S. Cherkasov, and V. I. Shirokov, *Opt. Spectrosc.* **19**, 39 (1965).
13. W. R. Ware, S. K. Lee, G. J. Brant, and P. P. Chow, *J. Chem. Phys.* **54**, 4729 (1970).
14. J. H. Easter, R. P. De Toma, and L. Brand, *Biophys. J.* **16**, 571 (1976).
15. M. G. Badea, R. P. De Toma, and L. Brand, *Biophys. J.* **24**, 197 (1978).
16. J. R. Lakowicz, H. Cherek, G. Laczko, and E. Gratton, *Biochim. Biophys. Acta* **777**, 193 (1984).
17. M. Maroncelli, J. MacInnis, and G. R. Fleming, *Science* **243**, 1674 (1989).
18. G. R. Fleming and P. G. Wolynes, *Phys. Today* **43**, 36 (1990).
19. E. W. Castner Jr., G. R. Fleming, B. Bagchi, and M. Maroncelli, *J. Chem. Phys.* **89**, 3519 (1988).
20. I. Rips, J. Klafter, and J. Jortner, *J. Chem. Phys.* **89**(7), 4288 (1988).
21. J. Hubbard and L. Onsager, *J. Chem. Phys.* **67**, 4850 (1977).
22. S.-G. Su and J. D. Simon, *J. Phys. Chem.* **91**, 2693 (1987).
23. W. Jarzeba, G. C. Walker, A. E. Johnson, M. A. Kahlow, and P. F. Barbara, *J. Phys. Chem.* **92**, 7039 (1988).
24. E. Görlach, H. Gygax, P. Lubini, and U. P. Wild, *Chem. Phys.* **194**, 185 (1995).
25. O. A. Karim, A. D. J. Haumet, M. J. Banet, and J. D. Simon, *J. Phys. Chem.* **92**, 3391 (1988).
26. R. M. Levy, D. B. Kitchen, J. T. Blair, and K. Krogh-Jespersen, *J. Phys. Chem.* **94**, 4470 (1990).
27. M. A. Kahlow, W. Jarzeba, T. J. Kang, and P. F. Barbara, *J. Chem. Phys.* **90**(1), 151 (1988).
28. E. W. Castner, B. Bagchi, M. Maroncelli, S. P. Webb, A. J. Ruggiero, and G. R. Fleming, *Ber. Bunsenges Phys. Chem.* **92**, 363 (1988).
29. E. W. Castner, M. Maroncelli, and G. R. Fleming, *J. Chem. Phys.* **86**(3), 1090 (1986).
30. L. Van Dommelen, N. Boens, F. C. De Schryver, and M. Ameloot, *J. Phys. Chem.* **99**, 8959 (1995).
31. J. R. Lakowicz, J. Kuśba, I. Gryczynski, W. Wiczk, H. Szmacinski, and M. L. Johnson, *J. Phys. Chem.* **95**, 9654 (1991).
32. J. R. Lakowicz, G. Laczko, and I. Gryczynski, *Rev. Sci. Instrum.* **57**, 2499 (1986).
33. H. Kasai, M. Goto, K. Iheda, M. Zama, Y. Mizuno, S. Takemura, T. Sugimoto, and T. Goto, *Biochemistry* **15**, 898 (1976).
34. I. Gryczynski, A. Kawski, K. Nowaczyk, S. Paszyc, and B. Skalski, *Biochem. Biophys. Res. Commun.* **98**, 1070 (1981).
35. J. R. Lakowicz, G. Laczko, H. Cherek, E. Gratton, and M. Limkeman, *Biophys. J.* **46**, 463 (1984).
36. E. Gratton, J. R. Lakowicz, B. Maliwal, H. Cherek, G. Laczko, and M. Limkeman, *Biophys. J.* **46**, 479 (1984).
37. I. Gryczynski, J. Czajko, S. Pasczyc, and B. Skalski, *Acta Phys. Chem. (Szeged, Hungary)* **29**, 113 (1983).
38. G. Weber and J. R. Lakowicz, *Chem. Phys. Lett.* **22**, 419 (1973).
39. J. R. Lakowicz and D. Hogen, *Biochemistry* **20**, 1366 (1981).
40. J. R. Lakowicz and A. Balter, *Biophys. Chem.* **16**, 117 (1982).
41. J. R. Lakowicz, M. L. Johnson, N. Joshi, G. Laczko, and I. Gryczynski, *Chem. Phys. Lett.* **131**, 343 (1986).

42. P. S. Eis, J. Kusba, M. L. Johnson, and J. R. Lakowicz, *J. Fluoresc.* **3**, 23 (1993).
43. A. Gafni and L. Brand, *Chem. Phys. Lett.* **58**, 346 (1978).
44. J. R. Laws and L. Brand, *J. Phys. Chem.* **83**, 795 (1979).
45. J. R. Lakowicz and A. Balter, *Biophys. Chem.* **16**, 99 (1982).
46. S. K. Gard and C. P. Smyth, *J. Phys. Chem.* **69**, 1294 (1965).
47. I. Gryczynski, H. Cherek, and J. R. Lakowicz, *Biophys. Chem.* **30**, 271 (1988).
48. I. Gryczynski, S. Paszyc, W. M. Wiczk, G. Laczko, N. Joshi, H. Szmacinski, and H. Cherek, *Z. Naturforsch.* **46**, 269 (1990).
49. E. W. Castner, G. R. Fleming, and B. Bagchi, *Chem. Phys. Lett.* **143**(3), 270 (1988).
50. H. Fellner-Feldegg, *J. Phys. Chem.* **75**, 616 (1969).
51. D. W. Davidson and R. H. Cole, *J. Chem. Phys.* **19**(12), 484 (1951).
52. D. J. Denny and R. H. Cole, *J. Chem. Phys.* **23**(10), 1767 (1955).